Mon. Not. R. Astron. Soc. **339,** 993–1005 (2003)

The interaction of a giant planet with a disc with MHD turbulence – II. The interaction of the planet with the disc

Richard P. Nelson★ and John C. B. Papaloizou
Astronomy Unit, Queen Mary, University of London, Mile End Road, London E1 4NS

Accepted 2002 October 31. Received 2002 October 30; in original form 2002 August 6

ABSTRACT

We present a global magnetohydrodynamics (MHD) simulation of a turbulent accretion disc interacting with a giant protoplanet of 5 Jupiter masses in a fixed circular orbit. The disc model had an aspect ratio $H/r = 0.1$, and in the absence of the protoplanet a typical value of the Shakura–Sunyaev stress parameter $\alpha = 5 \times 10^{-3}$. As expected from previous work, the protoplanet was found to open and maintain a significant gap in the disc, with the interaction leading to inward migration of the protoplanet orbit on the expected time-scale. No evidence for a persistent net mass flow through the gap was found. However, this may be because an extensive inner cavity could not be formed for the model adopted.

Spiral waves were launched by the protoplanet and, although these appeared to be diffused and dissipated through interaction with the turbulence, they produced an outward angular momentum flow which compensated for a reduced flux associated with the MHD turbulence near the planet, so maintaining the gap.

When compared with laminar disc models, with the same estimated α in the absence of the planet, the gap was found to be deeper and wider, indicating that the turbulent disc behaved as if it in fact possessed a smaller α, even though analysis of the turbulent stress indicated that it was not significantly affected by the planet in the region away from the gap. This may arise for two reasons. First, unlike a Navier–Stokes viscosity with anomalous viscosity coefficient, the turbulence does not provide a source of constantly acting friction in the near vicinity of the planet that leads to steady mass flow into the gap region. Instead, the turbulence is characterized by large fluctuations in the radial velocity, and time averaging of these fluctuations over significant time-scales is required to recover the underlying mass flow through the disc. In the vicinity of the planet, the disc material experiences high amplitude periodic perturbations on time-scales that are short relative to the time-scale required for averaging. Consequently the disc response is likely to be significantly altered relative to that expected from a Navier–Stokes model. Secondly, the simulation indicates that an ordered magnetic connection between the inner and outer disc can occur enabling angular momentum to flow out across the gap, helping to maintain it independently of the protoplanet's tide. This type of effect may assist gap formation for smaller mass protoplanets which otherwise would not be able to maintain them.

There is also some evidence that magnetic connection between the circumstellar disc and material that flows into the protoplanet's Hill sphere may lead to significant magnetic braking of the resulting circumplanetary disc, thereby modifying the expected gas accretion rate on to forming gas giant planets.

Key words: accretion, accretion discs – instabilities – MHD – turbulence – planetary systems: formation – planetary systems: protoplanetary discs.

★E-mail: R.P.Nelson@qmul.ac.uk

1 INTRODUCTION

The recent and ongoing discovery of extrasolar giant planets has stimulated renewed interest in the theory of planet formation (e.g. Mayor & Queloz 1995; Marcy, Cochran & Mayor 2000; Vogt et al. 2002). At the present time, there are two main competing theories for the formation of giant gas-rich planets, both of which assume formation in a protostellar disc. In the first, giant planets are envisaged to form directly from the gravitational fragmentation of a young protostellar disc (e.g. Boss 2001). In the second, giant planets form by the gradual buildup of a rocky core through coagulation of solids, and this core undergoes significant gas accretion once the core mass reaches $\simeq$15 Earth masses (e.g. Bodenheimer & Pollack 1986; Pollack et al. 1996). In either scenario, the gravitational interaction between the protoplanet and the protostellar disc from which it forms will play an important role in subsequent evolution.

There have been a number of studies of disc–protoplanet interaction. In the standard picture, a protoplanet exerts torques on a protostellar disc through the excitation of spiral density waves at Lindblad resonances (e.g. Goldreich & Tremaine 1979), and these waves carry with them an associated angular momentum flux. This angular momentum is deposited in the disc material where the waves are damped, leading to an exchange of angular momentum between protoplanet and disc. The planet exerts a positive torque on the disc that lies exterior to its orbit and a negative torque on the interior disc.

Previous studies of the interaction between a protoplanet and a viscous disc (Papaloizou & Lin 1984; Lin & Papaloizou 1993) indicate that a sufficiently massive protoplanet can open up an annular gap in the disc about the planet's orbital radius provided: (i) the tidal torque due to the planet is greater than the internal viscous torque; (ii) the spiral density waves excited by the planet form shocks, ensuring that the torque exerted by the planet is applied locally to the disc (Ward 1997). For most protostellar disc models, the protoplanet needs to be approximately a Jovian mass for gap formation to occur. Recent simulations (Bryden et al. 1999; Kley 1999; Lubow, Seibert & Artymowicz 1999; D'Angelo, Henning & Kley 2002) examined the formation of gaps by giant protoplanets, and also estimated the gas accretion rate on to the planets. The detailed form of the gaps, and by association the gas accretion rate on to the protoplanet, is found to be a function of the viscosity in the disc, as well as the planet mass and the disc vertical scale height, H. The orbital evolution of a Jovian mass protoplanet embedded in a standard viscous protostellar disc model was studied by Nelson et al. (2000), who showed that gap formation leads to the creation of a low-density inner cavity in which the planet orbits, and that continued interaction with the outer disc leads to inwards migration on a time-scale of a few $\times 10^5$ yr. It was estimated that a Jovian mass protoplanet would increase its mass to $\sim$3 Jupiter masses by accretion of gas from the disc for this time. The disc models in these studies all modelled the disc viscosity through the Navier–Stokes equation, using an α model for the kinematic viscosity.

Until quite recently, most models of viscous accretion discs used the α model of Shakura & Sunyaev (1973) for the anomalous disc viscosity. This assumes that the viscous stress is proportional to the thermal pressure in the disc without specifying the origin of the viscous stress (but assumed to arise from some form of turbulence). Work by Balbus & Hawley (1991) indicated that significant angular momentum transport in weakly magnetized discs could arise from the magnetorotational instability (MRI) – or the Balbus–Hawley instability. Subsequent non-linear numerical simulations, performed using a local shearing box formalism (e.g. Hawley & Balbus 1991; Hawley, Gammie & Balbus 1996; Brandenburg et al. 1996), confirmed this and showed that the saturated non-linear outcome of the MRI is magnetohydrodynamics (MHD) turbulence with an associated viscous stress parameter α of between $\sim 5 \times 10^{-3}$ and $\sim$0.1, depending on the initial magnetic field configuration. More recent global simulations of MHD turbulent discs (e.g. Armitage 1998; Hawley 2000, 2001; Steinacker & Papaloizou 2002) confirm the picture provided by the local shearing box simulations.

In a companion paper to this one (Papaloizou & Nelson 2003, hereafter Paper I, this issue) we present the results of three-dimensional (3D) global MHD simulations of turbulent discs initiated with zero net flux magnetic fields. We examine the behaviour of the discs as a function of varying the disc scale height, H, the extent of the radial domain, the numerical resolution, and the initial magnetic field configuration (poloidal or toroidal). We find that these disc models produce volume averaged values for the stress parameter $\alpha \sim 5 \times 10^{-3}$. We note that this value is typical of that expected in protostellar discs to maintain the canonical mass accretion rate of 10^{-8} $M_\odot$ yr $^{-1}$ on to T Tauri stars (e.g. Hartmann et al. 1998). We also consider the issue of time averaged estimates for the radial distribution of turbulent quantities, such as the time averaged stress parameter α and the time averaged mass flux through the disc. Balbus & Papaloizou (1999) noted the need to consider time averages of these quantities in order to connect the behaviour of MHD turbulent discs models with standard viscous accretion disc theory. Indeed, we find reasonable agreement between the expectations of viscous disc theory and the results of the simulations in Paper I, when appropriate time averages are considered. One of the models presented in Paper I (model E) was used as the basis for the work presented in this paper.

The calculations presented in this paper and in Paper I assume that the equations of ideal MHD apply. Questions have been raised concerning the degree of ionization in protostellar discs (e.g. Gammie 1996), and thus about the applicability of the equations of ideal MHD in the modelling of protoplanetary discs. This is a complex issue that has yet to be fully resolved, so we assume that the equations of ideal MHD are a valid approximation in these first papers on the interaction between turbulent discs and embedded protoplanets. Future work will address the issue of the ionization fraction in protostellar discs, and the effects this may have on disc–planet interactions.

Significant work has already been done on examining the interaction between giant protoplanets and viscous protostellar discs using laminar α disc models. The improvement and availability of high-performance computing resources has now made it possible to develop global models of MHD turbulent discs in which the underlying mechanism responsible for angular momentum transport is explicitly calculated. The next important step in understanding the interaction between protostellar accretion discs and embedded giant protoplanets is to compute models of turbulent MHD discs interacting with giant protoplanets. This is the subject of the present paper.

The underlying disc model that we consider (described in detail in Paper I) has a constant ratio of disc scale height to radius of $H/r = 0.1$, and a volume and time averaged value of the stress parameter $\alpha = 5 \times 10^{-3}$. In order for a protoplanet to form a gap in such a disc, it must have a mass of at least 3 Jupiter masses (assuming the central stellar mass is 1 $M_\odot$) according to the thermal criterion (see Section 3.2). In order to be certain of generating a clean gap, we consider a protoplanet with 5 Jupiter masses. We note that, at the present time, it is beyond our computational resources to consider thinner discs and lower mass planets. Protostellar discs are more typically expected to have $H/r = 0.05$, but to model such discs

would require a doubling of the number of grid cells in each direction. We have found from conducting numerical experiments that zero net magnetic flux disc models require a numerical resolution similar to that we consider here in order to sustain MHD turbulence at a reasonable level, and to generate reasonable values of α. Ideally we would wish to perform simulations of discs with $H/r = 0.05$ and Jovian mass protoplanets. However, we believe that the results obtained will still provide a reliable picture of how protoplanets interact with turbulent discs.

In particular, as expected from previous work, the protoplanet was found to open and maintain a significant gap in the disc, with the interaction leading to inward migration of the protoplanet orbit on the expected time-scale. Spiral waves were launched by the protoplanet producing an outward angular momentum flow and reducing that provided by the MHD turbulence near the planet. The turbulent disc behaved as if it possessed a smaller α than expected. The characteristic flow induced by the protoplanet was found to facilitate an ordered magnetic connection between the inner and outer disc enabling angular momentum to flow out across the gap. This effect provides an additional mechanism for maintaining the gap and may account for the apparently smaller α, along with the fact that the turbulence does not provide a source of constantly acting friction, unlike a Navier–Stokes viscosity.

The plan of the paper is as follows. In Sections 2 and 2.1 we described our initial model set-up and numerical procedure. In Section 3.1 we discuss the issue of time averaging, the relevant disc quantities and the connection to standard viscous disc theory. In Section 3.2, we discuss the basic ideas of disc–protoplanet interactions, and our expected results based on this previous work. In Section 3.3, we discuss the time-dependent evolution of the model, and in Section 3.4 we compare our results with those obtained from laminar viscous disc models. Finally, in Section 4 we discuss our results and draw our conclusions.

2 INITIAL MODEL SET-UP

The governing equations for MHD written in a frame rotating with a uniform angular velocity $\Omega_{\rm p}\hat{\boldsymbol{k}}$ (with $\hat{\boldsymbol{k}}$ being the unit vector in the vertical direction) are

$$\frac{\partial \rho}{\partial t} + \nabla \cdot \rho \boldsymbol{v} = 0, \tag{1}$$

$$\rho\left(\frac{\partial \boldsymbol{v}}{\partial t} + \boldsymbol{v}\cdot\nabla\boldsymbol{v}\right) + 2\Omega_{\rm p}\hat{\boldsymbol{k}}\times\boldsymbol{v} = -\nabla p - \rho\nabla\Phi + \frac{1}{4\pi}(\nabla\times\boldsymbol{B})\times\boldsymbol{B}, \tag{2}$$

$$\frac{\partial \boldsymbol{B}}{\partial t} = \nabla\times(\boldsymbol{v}\times\boldsymbol{B}) \tag{3}$$

where $\boldsymbol{v}$, P, ρ, $\boldsymbol{B}$ and Φ denote the fluid velocity, pressure, density, magnetic field and potential, respectively.

The angular velocity $\Omega_{\rm p}$ corresponds to that of a planet in fixed circular orbit at radius D. The perturbing planet thus appears stationary in the chosen reference frame. The potential Φ contains contributions due to gravity and the centrifugal potential $-(1/2)\,\Omega_{\rm p}^2\,r^2$. We use a locally isothermal equation of state

$$P(r) = c(r)^2\rho, \tag{4}$$

where $c(r)$ denotes the sound speed which is specified as a fixed function of r.

The disc model investigated may be described as a cylindrical disc (e.g. Hawley 2001) and has been considered prior to the introduction of a perturbing planet in Paper I as model E. This disc model was such that $c(r)/r\Omega(r) = 0.1$, so that the effective ratio of disc scale height to radius $H/r = 0.1$, and had a volume averaged value of the stress parameter $\alpha \simeq 5\times10^{-3}$. We adopt cylindrical coordinates (z, r, ϕ) based on the centre of mass of the central star plus protoplanet system. The number of grid cells used was $(N_r, N_\phi, N_z) = (370, 580, 60)$. The gravitational potential is due to the central star and internally orbiting planet. Thus we have

$$\Phi = -\frac{GM_*}{|\boldsymbol{r}-\boldsymbol{r}_*|} - \frac{Gm_{\rm p}}{\sqrt{r^2+D^2-2rD\cos(\phi-\phi_{\rm p})+b^2}} - \frac{1}{2}\Omega_{\rm p}^2 r^2. \tag{5}$$

The first term represents the gravitational potential due to the central star, with G being the gravitational constant and M_* being the stellar mass. The second term is the gravitational potential due to a planet in circular orbit at radius D and azimuthal angle $\phi_{\rm p}$ with a mass $m_{\rm p}$. The final term represents the centrifugal potential. To avoid a singularity in the planet potential, we adopt a softening parameter $b = R_{\rm H}/2$ where $R_{\rm H} = D(m_{\rm p}/3M_*)^{1/3}$ is the Hill sphere radius of the protoplanet. This enables a Roche lobe filling atmosphere to be set up around the protoplanet before the gap construction process is completed. Material flowing in the neighbourhood of the protoplanet then has to move around it and cannot be accreted. We thus cannot simulate the accretion of gas on to the protoplanet in this work. In previous work on disc–planet interactions (e.g. Nelson et al. 2000), accretion of gas by a protoplanet is modelled by simply removing matter from within the Roche lobe at a specified rate. A technical difficulty arises in a simulation such as that presented here which includes magnetic fields, becasue we also have to consider what happens to the magnetic field when gas is accreted by the protoplanet. This is the primary reason why we do not explicitly calculate the gas accretion rate on to the protoplanet in this work.

In this paper we consider the time-dependent evolution of a turbulent disc together with a planet with $m_{\rm p}$ equal to *5* Jupiter masses. We initially immerse the planet at $r \equiv D = 2.2$ and $\phi_{\rm p} = \pi$ into a fully turbulent disc model covering the full azimuthal domain of 2π. The initial model we adopt is model E, which has been described in Paper I. When a planet is immersed directly into such a model, we find that large-scale transients occur which prevent the efficient and quick formation of a gap. It was not possible to follow such transients to a conclusion in a run of reasonable duration. To avoid such problems, we carved out a gap in the density profile centred on the planet's radial location before inserting the planet. This had the effect of perturbing the disc from a steady state, so it was allowed to relax until a steady state had been reattained. The planet was then inserted into the disc and the calculation initiated with the time t being reset to zero. We comment that, in carving out the initial gap, the magnetic field was not altered. This means that the magnetic energy in the initial gap would be significantly larger than expected for relaxed turbulence under conditions of zero net flux. However, the runs were subsequently continued for about 100 planet orbits, which is significantly longer than the time required for adjustment of the local turbulence (see Paper I). Furthermore, after such times, the magnetic stresses appeared to have reached a steady pattern and to be largely associated with magnetic field concentrated into wakes which were absent when the planet was initially inserted. Thus, the behaviour of the magnetic field in the gap region is not determined by the conditions prevailing when the gap was set up.

A test run was performed in the absence of an embedded protoplanet to ensure that the turbulent disc relaxed to a state with the expected magnetic energy once an initial gap had been carved out.

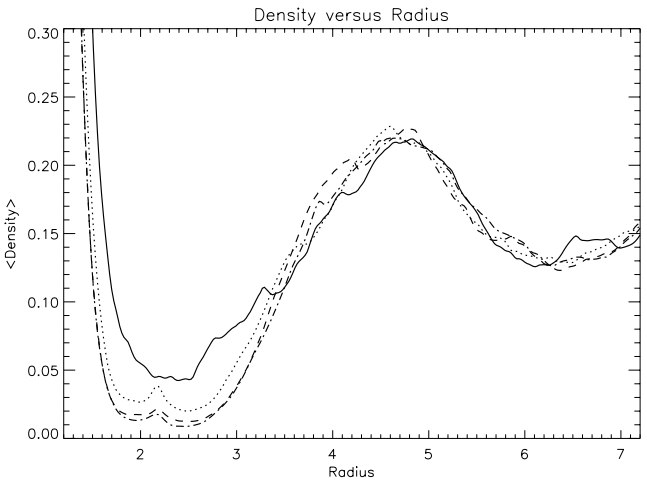

Figure 1. The azimuthally averaged density at the vertical midplane of the disc is plotted as a function of radius at $t = 0$ (solid line). The remaining curves correspond to the same physical quantity after times of $t = 675.6$ (dotted line), $t = 1351.2$ (dashed line) and $t = 2047.28$ (dot-dashed line). These times correspond to 0, 33, 66 and 100 orbits of the protoplanet, respectively. Note that the initial gap has been deepened and widened considerably. Also some accretion into the central regions has occurred.

The results of this run showed that the disc returns to its normal turbulent state within a few orbits.

In Fig. 1 we plot the form of the azimuthally averaged density profile located at the vertical midplane of the disc at the stage when the planet is introduced.

As in Paper I, units are adopted such that $r_1 = 1$ and $GM = 1$, where r_1 is the radius of the inner radial boundary of the computational domain. We note that a single simulation of this type requires of the order of 30 000 CPU hours on an Origin 3800 parallel processing facility.

2.1 Numerical procedure

The numerical scheme that we employ is based on a spatially second-order accurate method that computes the advection using the monotonic transport algorithm (Van Leer 1977). The MHD section of the code uses the method of characteristics constrained transport (MOCCT) as outlined in Hawley & Stone (1995) and implemented in the ZEUS code. The code has been developed from a version of NIRVANA originally written by Ziegler (Ziegler & Rüdiger 2000).

3 NUMERICAL RESULTS

Before describing results in detail, we discuss some average quantities used in their description.

3.1 Vertically and horizontally averaged stresses, angular momentum transport and external torques

For a global coarse grained description of the flow, as in Paper I, we use quantities that are both vertically and azimuthally averaged over the (ϕ, z) domain (e.g. Hawley 2000) and, in some cases, an additional time average. Adopting the same formalism and notation as in Paper I, we write the vertically and azimuthally averaged continuity equation in the form

$$\frac{\partial \Sigma}{\partial t} + \frac{1}{r}\frac{\partial\,(r\,\Sigma\overline{v_r})}{\partial r} = 0, \tag{6}$$

where the disc surface density is given by

$$\Sigma = \frac{1}{2\pi}\int \rho\,\mathrm{d}z\,\mathrm{d}\phi. \tag{7}$$

We adopt the α stress parameter of Shakura & Sunyaev (1973) appropriate to the total stress as defined in Paper I. Then the vertically and azimuthally averaged azimuthal component of the equation of motion can be written in the form

$$\frac{\partial(\Sigma\overline{j})}{\partial t} + \frac{1}{r}\left(\frac{\partial(r\,\Sigma\overline{v_r}\,\overline{j})}{\partial r} + \frac{\partial(\Sigma r^2\alpha\overline{P/\rho})}{\partial r}\right)$$

$$= -\int \rho\frac{\partial\Psi}{\partial\phi}\,\frac{\mathrm{d}\phi\,\mathrm{d}z}{2\pi}. \tag{8}$$

Here $j = r v_\phi$ is the specific angular momentum and the term on the right-hand side represents the azimuthally and vertically integrated torque acting on the disc (absent in Paper I), which is here due to the internally orbiting planet. Note that this form is identical to that obtained in standard viscous disc theory (see Balbus & Papaloizou 1999).

Equations (6) and (8) may be used with or without a time averaging procedure in addition to horizontal and vertical averaging (see Paper I).

3.2 Disc–planet interactions and gap formation

In the usual picture of disc–protoplanet interactions, the presence of a protoplanet orbiting in a gaseous accretion disc leads to the excitation of spiral density waves at Lindblad resonances, which propagate from the locations where they are launched (e.g. Goldreich & Tremaine 1979). These spiral waves carry with them an associated angular momentum flux which is deposited in the disc where the waves are damped, either through shocks or viscous effects.

Previous work on the interaction between a giant protoplanet and a viscous protoplanetary disc indicates that an annular gap is expected to form in the vicinity of the protoplanet provided that two criteria are satisfied (e.g. Lin & Papaloizou 1993). The first criterion (the so-called viscous criterion) requires that

$$\frac{m_\mathrm{p}}{M_*} > 40\alpha\left(\frac{H}{R}\right)^2 \tag{9}$$

which arises from the requirement that tidal torques induced by the protoplanet exceed viscous torques in the disc. The second criterion (the so-called thermal criterion) requires that

$$\frac{m_\mathrm{p}}{M_*} > 3\left(\frac{H}{R}\right)^3 \tag{10}$$

and comes from the requirement that the spiral waves introduced into the disc flow by the planet be non-linear so that spiral shocks form (Ward 1997).

The disc model that we employ in this work is characterized by a value of $H/R = 0.1$ and a volume averaged value of $\alpha \simeq 0.005$ (see Paper I). It is thus expected that the presence of a 5 Jupiter mass protoplanet will lead to gap clearing. Previous numerical work on disc–protoplanet interactions (Nelson et al. 2000) suggests that gap formation in a disc in which the gas can accrete on to a central star will lead to the eventual formation of a low-density inner cavity. We note that our use of an inner boundary layer in this work will prevent an extensive cavity from forming.

3.3 Time-dependent evolution of the model

The disc model together with the planet was run for 2040 time units. This corresponds to ∼324 orbits at $r = 1$, about 100 orbits

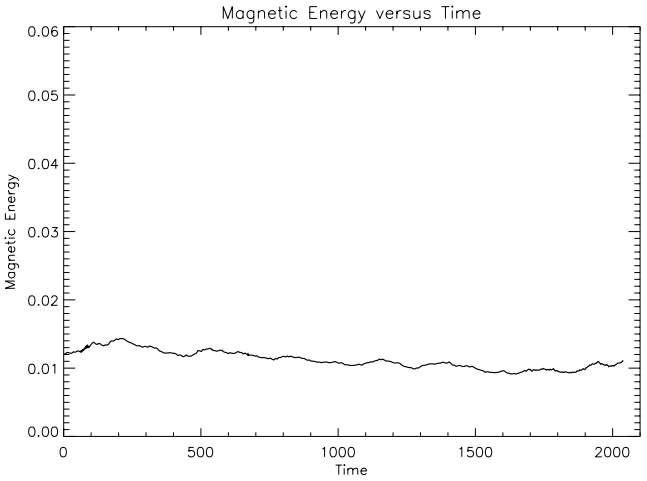

Figure 2. Magnetic energy in the Keplerian domain expressed in units of the volume integrated pressure as a function of time. Note that the value of ∼0.01 is very similar to that obtained in the absence of the protoplanet.

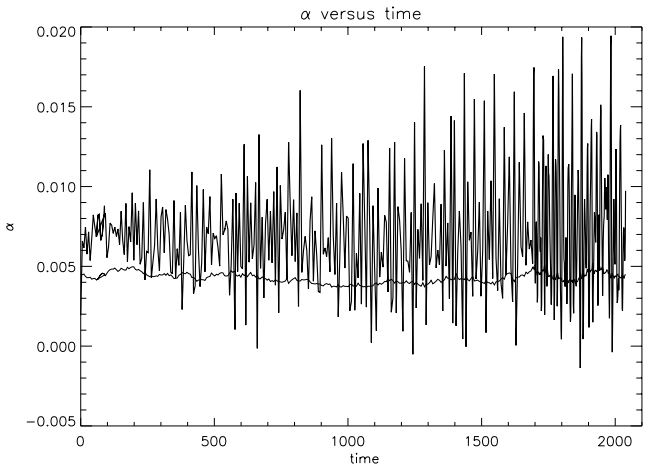

Figure 3. The stress parameter α volume averaged over the Keplerian domain is plotted as a function of time. The upper curve is derived from the total stress while the lower curve is derived from the magnetic contribution.

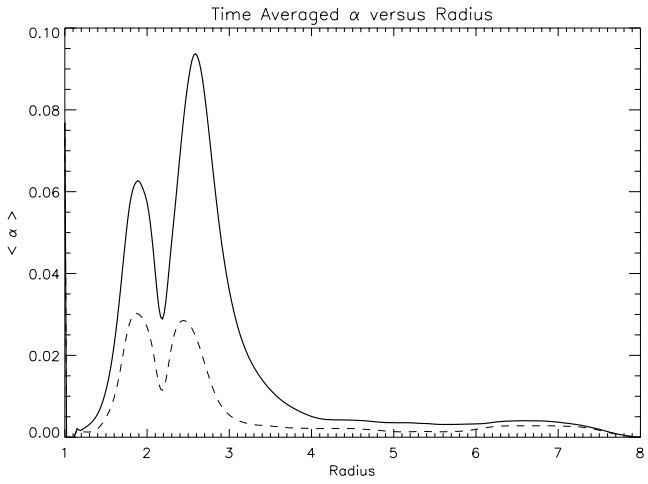

Figure 4. A time average of the vertically and azimuthally averaged value of the stress parameter α plotted as a function of dimensionless radius. The solid curve corresponds to the combined effects of magnetic and Reynolds stresses, whereas the dashed curve gives the contribution from magnetic stresses alone. The average is taken between time $t = 1650.0$ and 2040.0.

at $r = 2.2$ (where the planet is located), and about 17 orbits at $r = 7.2$. We found that the initial gap considerably deepened, and accretion on to the central parts occurred producing something like a central cavity seen in previous work (e.g. Nelson et al. 2000). We note that this cannot become very extensive in the present work because of our adoption of an inner boundary layer which prevents mass from flowing through the inner boundary. The behaviour of the azimuthally averaged value of $\rho(r)$ at the disc midplane throughout the run is indicated in Fig. 1.

Throughout the run, MHD turbulence is sustained in regions of the disc not strongly affected by the planet. However, the planet has a large enough mass to strongly perturb the disc locally generating outward and inward propagating density waves as well as extending the initial gap, as expected from the discussion in Section 3.2.

The magnetic energy in the Keplerian domain expressed in units of the volume integrated pressure is given as a function of time in Fig. 2. A value of ∼0.01 is maintained throughout. This is similar to what is found for models without the planet, and indicates that the perturbing presence of the protoplanet does not have a strong effect on the dynamo operating *globally* within the disc. However, there is evidence that the protoplanet affects the turbulence locally, creating an ordered field where the material passes through the spiral shocks in the gap region.

The stress parameter α volume averaged over the Keplerian domain is plotted as a function of time in Fig. 3. The magnetic contribution ∼0.004 is similar to that occurring without the planet. However, the typical total stress is much larger, reaching peak values of $\alpha \sim 0.02$. This is due to the large contribution of Reynolds stresses associated with the spiral waves launched by the protoplanet.

As in Paper I, we explore the behaviour of time averages of the stress parameter α and its variation with radius. Only in this way can we make a connection with earlier theories of gap formation in viscous discs. A time average of the stress parameter α taken between times $t = 1650.0$ and 2040.0 is plotted as a function of dimensionless radius in Fig. 4. Both the total stress parameter α and the magnetic contribution to it become large in the vicinity of the planet $r < 3$ where the gap is. This arises even though the actual magnetic stress $T_{\rm m} = B_r B_\phi / 4\pi$ decreases in the gap region once the gap is formed, as indicated by Fig. 5, because the pressure P in the gap decreases by an even larger fraction (note that magnetic stress parameter $\alpha = -T_{\rm m}/P$). Further away beyond $r > 5$–6, values similar to those pertaining to the disc without a planet are attained, indicating that the planet does not have a significant effect on the turbulence outside the gap region.

Inspection of equation (8), however, suggests we should consider the non-advected part of the angular momentum flux which is proportional to $r^2 \times$ stress or $\Sigma r^2 \alpha \overline{P/\rho}$ when discussing the disc evolution. We plot time averages of the angular momentum fluxes in Figs 5 and 6. The time averages for these are over the time intervals $1650 < t < 1920$ and $1650 < t < 2040$, respectively, and they both show the same behaviour. This indicates that a stable pattern of behaviour has been established relatively quickly.

This behaviour may be understood in the context of gap formation theory as applied to laminar discs with Navier–Stokes viscosity (e.g. Bryden et al. 1999). Consider equation (8) under the assumption of a disc in a quasi steady state with $\overline{v}_r = 0$. Suppose also there is a completely empty gap in which the planet is located. Then, equation (8) predicts that the angular momentum flux tends to a constant value

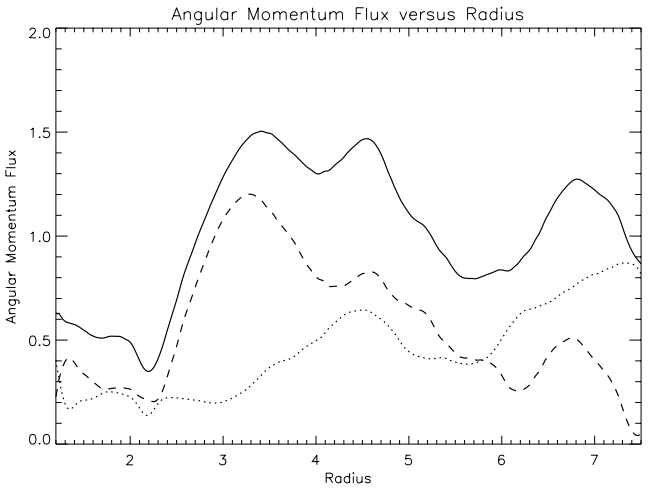

Figure 5. Time averages of the vertically and azimuthally averaged values of the non-advected part of the angular momentum flux in arbitrary units are plotted as a function of dimensionless radius. The solid line gives the total contribution from the magnetic plus Reynolds stress. The dashed line gives the Reynolds stress contribution and the dotted line gives the magnetic stress contribution. The average is taken between time $t = 1650.0$ and 1920.0.

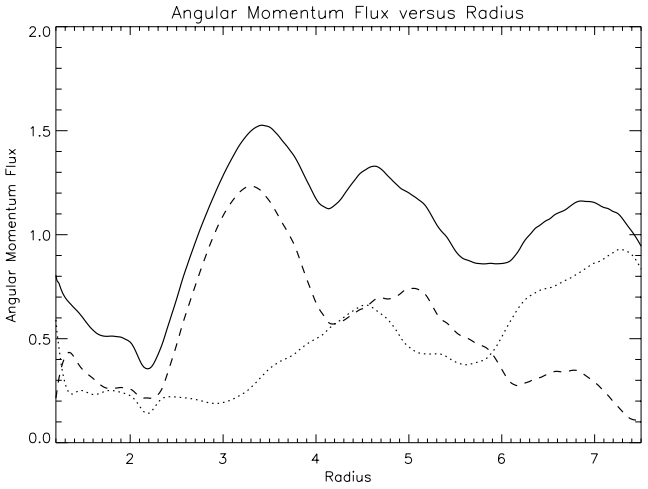

Figure 6. Time averages of the vertically and azimuthally averaged values of the non-advected part of the angular momentum flux in arbitrary units are plotted as a function of dimensionless radius. The solid line gives the total contribution from the magnetic plus Reynolds stress. The dashed line gives the Reynolds stress contribution and the dotted line gives the magnetic stress contribution. The average is taken between time $t = 1650.0$ and 2040.0.

at large distances from the planet. The flux is zero within the gap where there is no material, and is generated by the tidal torque term at the disc edge near the planet.

The behaviour of the fluxes illustrated in Figs 5 and 6 can be related to this expectation. We see that the total flux dips to a minimum at the location of the planet orbit and rises to an asymptotic value at large distances. The contribution from the Reynolds stresses initially rises, representing the generation of spiral waves by the protoplanet in the region of the gap wall and beyond, and reaches a maximum close to the outer 1:2 Lindblad resonance location, beyond which there is no further generation of spiral waves by a planet on a circular orbit. Beyond this region, the contribution from the Reynolds stresses decreases as these waves are dissipated. The magnetic contribution rises from a small but non-zero value near the planet to make most of the contribution at large radii. There, the behaviour is that of an unperturbed turbulent disc. The persistence of the magnetic stresses through the gap may be significant in that this can allow for the transmission of angular momentum from one side of the gap to the other without needing the contribution of a tidal torque from the planet. This may enhance the gap formation process with respect to what may be expected from non-magnetic laminar disc theory (see Section 3.4).

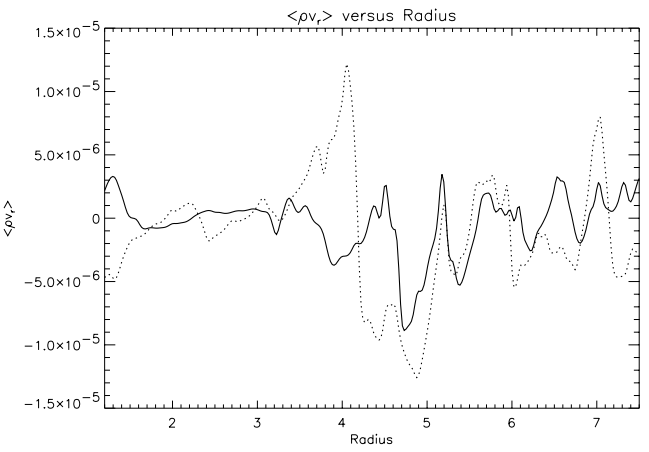

Figure 7. Time averages of the product of the vertically and azimuthally averaged values of Σ/L_z and v_r in arbitrary units are plotted as a function of dimensionless radius. For the solid curve the average is taken between time $t = 1650.0$ and 2040.0, while for the dotted curve it is taken between $t = 1650.0$ and 1920.0.

The angular momentum fluxes plotted in Figs 5 and 6 indicate a net outward value supplied by the planet's tide. This results in inward migration as has been verified by direct calculation of the torques acting on the planet itself. The torque, $\dot{J}$, arising from the disc beyond the planet orbital radius indicates an inward migration time defined by $J_{\rm planet}/\,J \simeq 2 \times 10^4$ planetary orbits, for a disc mass normalization such that there exist 2 Jupiter masses interior to the orbital radius of the planet $r_{\rm p} = 2.2$. Interestingly, the viscous timescale at the planet location defined by the usual expression $t_\nu = r^2/(\alpha\, H^2\, \Omega) \simeq 1.03 \times 10^4$ planetary orbits. It is clear that the planet undergoes inward migration at a rate that is in broad agreement with the expectations of type II migration theory (Lin & Papaloizou 1986, 1993; Nelson et al. 2000).

As in the unperturbed turbulent disc described in Paper I, the radial velocity shows large temporal fluctuations about a small mean value. However, in this case, when the planet is present the mean values tend to be smaller, giving some indication that planetary tides balance viscous transport. Time averages of the product of the vertically and azimuthally averaged values of Σ/L_z and v_r, in arbitrary units, are plotted as a function of dimensionless radius in Fig. 7. Here L_z is the extent of the vertical domain. The averages are taken between time $t = 1650.0$ and 1920.0 and between $t = 1650.0$ and 2040.0. Because of the small values, the two averages show significant deviation. None the less, the net mass flow is small. This is particularly the case interior to the planet where there is always a zero value at some radius near to $r = D$. This indicates no flow from the exterior of the planet to the interior for the duration of the averaging interval. Thus, while there is material within the gap, we see no evidence of a net flow through in this run. In this context, we note that results from laminar disc theory produce models in which significant mass flow through gaps may occur, as has been recently

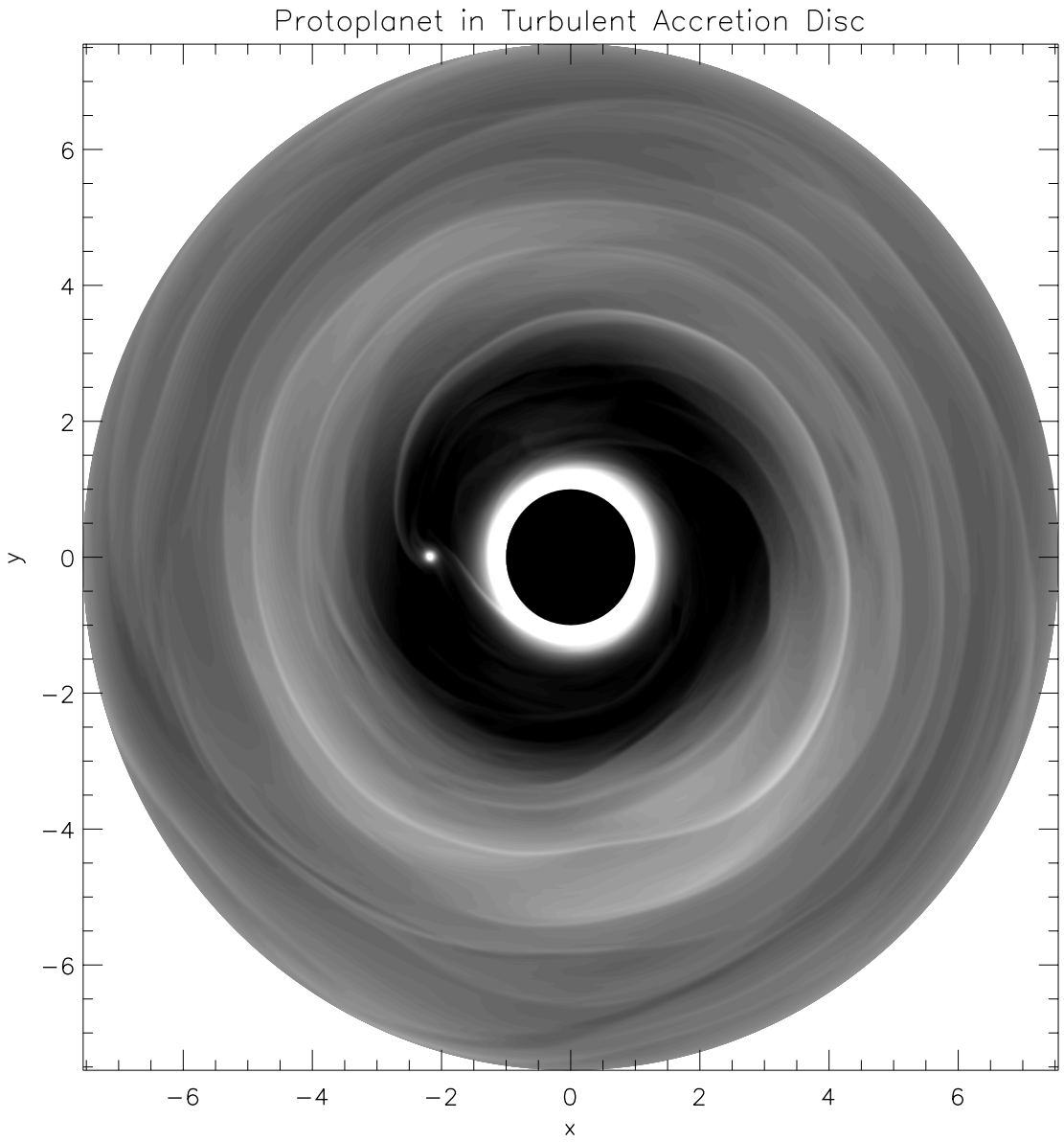

Figure 8. A typical contour plot for the midplane disc density at time $t = 1680.0$. The gap, planet and wakes it causes in the disc are apparent. The underlying turbulence has the effect of slightly blurring this picture relative to those obtained from simulations performed using laminar accretion discs with anomalous Navier–Stokes viscosities.

emphasized by Lubow et al. (1999). Our results suggest that different behaviour may be exhibited in an MHD turbulent disc, and indicate that the rate of mass accretion on to gap forming protoplanets may be smaller than is observed in laminar disc models.

The density distribution in the gap region resembles that obtained from laminar disc theory. A contour plot of the midplane density is given in Fig. 8. The wakes induced by the planet through the excitation of spiral waves are clearly visible. However, in this case because of the turbulence, they appear much less sharply defined than in the laminar disc case; see Nelson et al. (2000) and Fig. 16.

In the region of the wakes, the disc and its turbulence are strongly perturbed. Magnetic field vectors in the disc midplane in the neighbourhood of the planet are illustrated on different size scales in Figs 9 and 11, along with the corresponding density plots for the equivalent regions in Figs 10 and 12. An inspection of the magnetic field vectors indicates that these tend to line up along the location of the wakes but in a somewhat broadened region slightly behind the shocks. In this way, an ordered structure appears to be imposed on the flow and magnetic field by the protoplanet. The magnetic stress is largely communicated in these ordered regions as shown by Fig. 13, which shows a contour plot of the magnetic stress in the vicinity of the planet.

The velocity field within the Hill sphere of the planet is shown in the left-hand panel of Fig. 14 for the turbulent disc. An equivalent plot for a laminar disc is shown in the right-hand panel of this figure. The material that enters the Hill sphere of the protoplanet and becomes gravitationally bound to it is normally expected to circulate around it by virtue of its angular momentum. In the calculation presented here, the protoplanet does not accrete gas, and is modelled as a softened point mass. Consequently, it is expected that material which enters the Hill sphere will form a hydrostatic 'atmosphere' around the planet that is supported through pressure

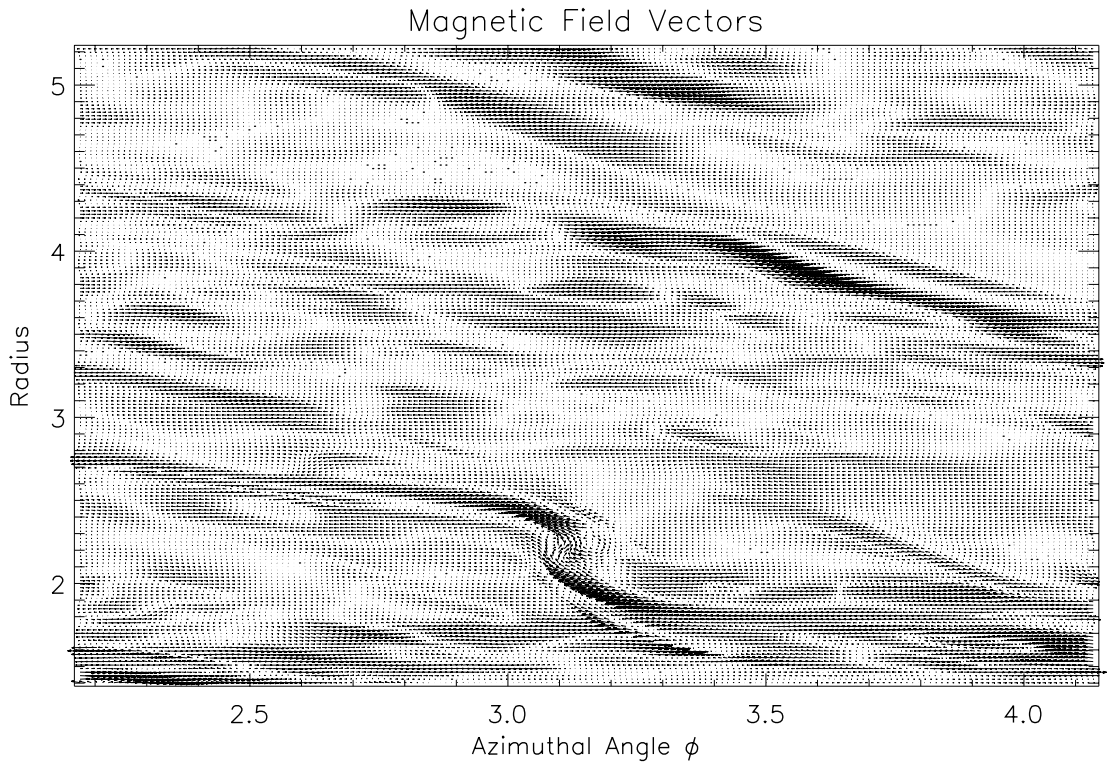

Figure 9. This figure shows the magnetic field vectors (B_r, B_ϕ) in the disc midplane plotted in the r–ϕ plane at time $t = 2040$. Note that the field is compressed and ordered in the vicinity of the wakes induced by the protoplanet.

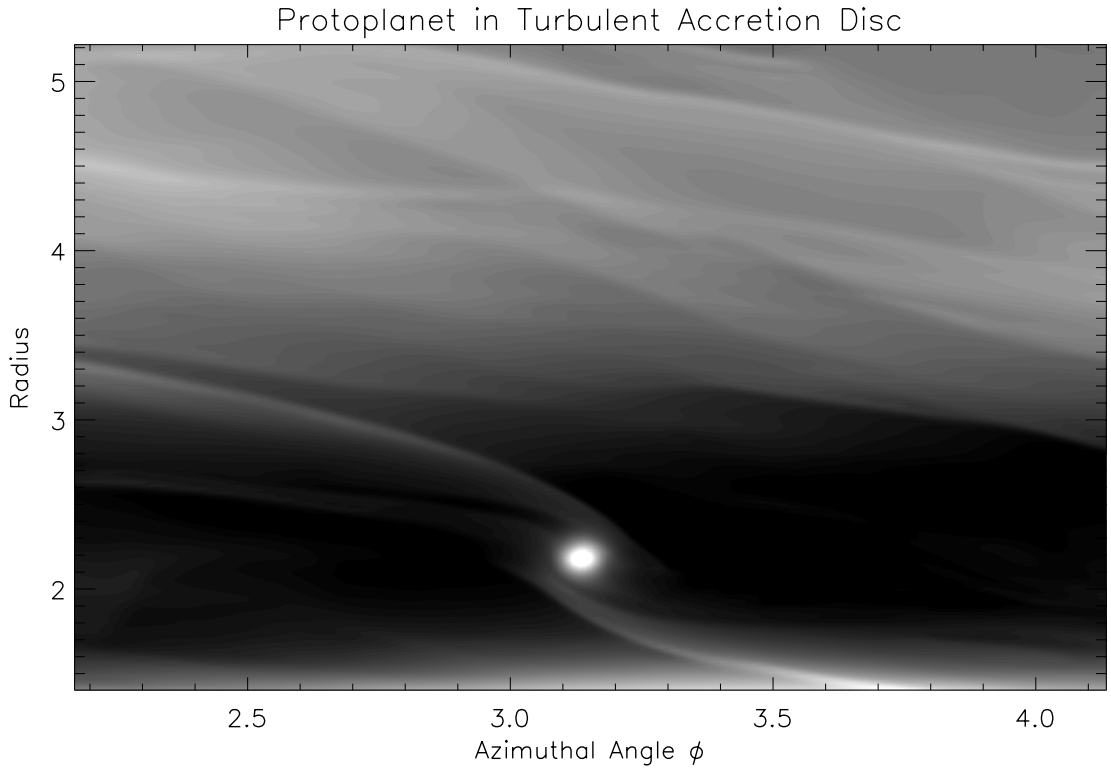

Figure 10. This figure shows the midplane density in the vicinity of the planet for an area that is the same as for the magnetic field plot in Fig. 9.

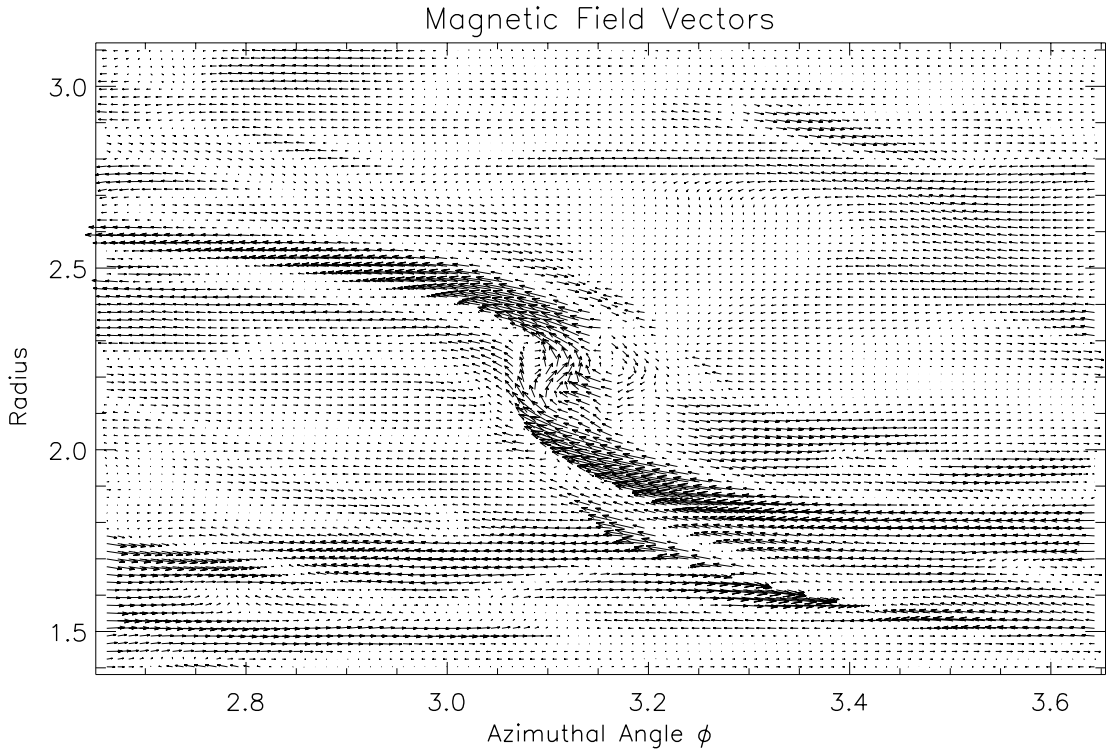

Figure 11. This figure shows the magnetic field vectors (B_r, B_ϕ) in the disc midplane plotted in the r–ϕ plane at time $t = 2040$ for an area that is smaller than that plotted in Fig. 9. It is clear that the field is ordered and compressed in the vicinity of the wakes induced by the protoplanet.

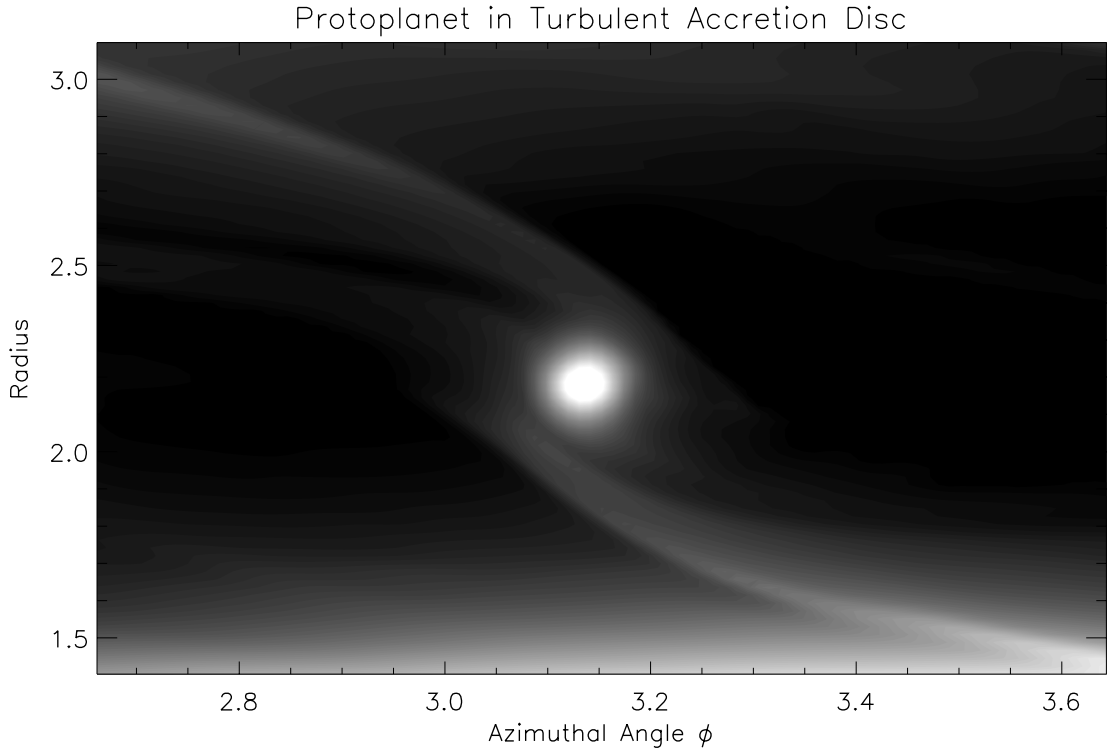

Figure 12. This figure shows density in the vicinity of the planet for an area equivalent to the magnetic field plot in Fig. 11.

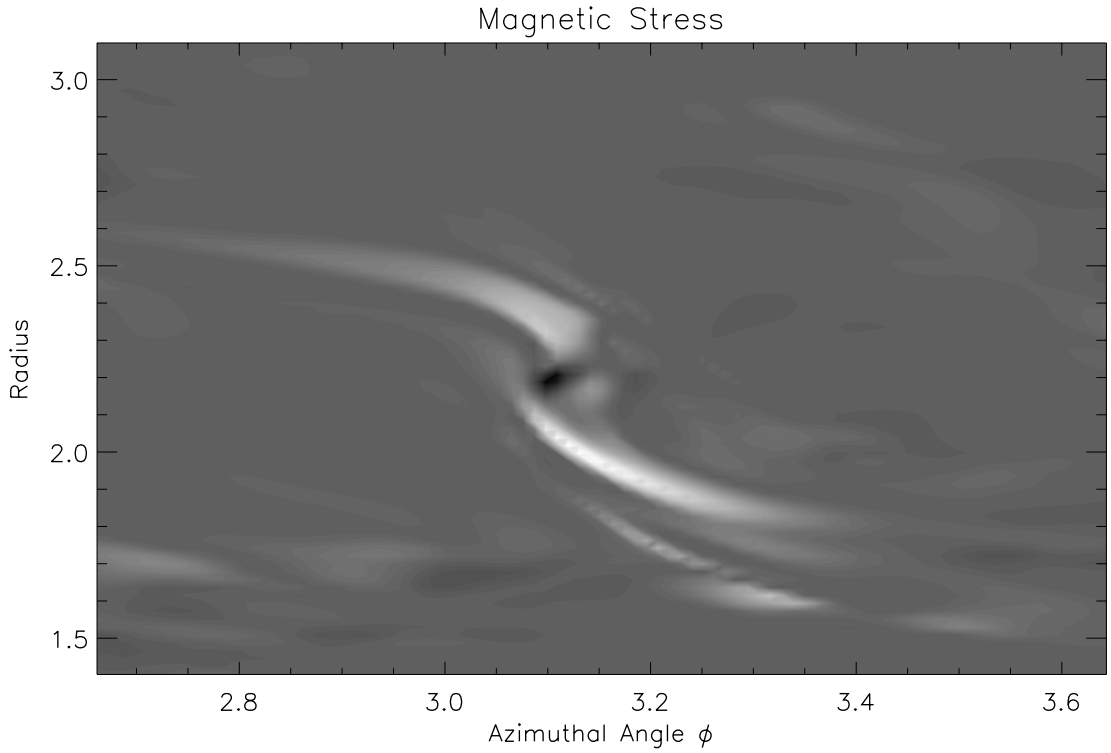

Figure 13. This figure shows the magnetic stress in the vicinity of the planet for an area equivalent to that shown in the magnetic field plot in Fig. 11. Note that the magnetic stress is greatest where the magnetic field is compressed and ordered just behind the wakes induced by the protoplanet.

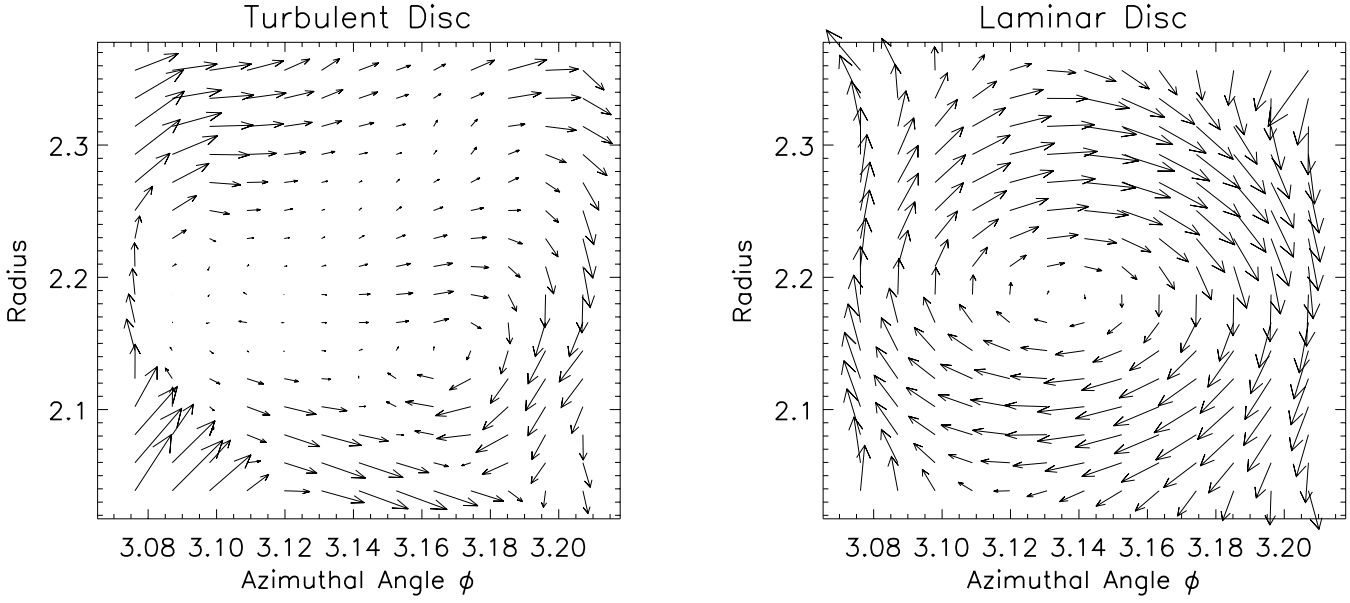

Figure 14. Velocity vectors in the disc midplane in the Hill sphere of the planet. The left-hand panel shows the results from the magnetized disc run, and the right-hand panel shows a laminar disc run with the same resolution. Note that the usual circulating pattern that is observed in the planet Hill sphere for non-magnetic disc–planet simulations is not apparent in the MHD turbulent case, for reasons discussed in the text.

and rotation. In Fig. 14 we would expect to see circulation occurring in a clockwise fashion for both the MHD turbulent disc and the laminar disc. However, it is apparent that the circulating pattern has been disrupted in the magnetized disc, indicating that magnetic braking may have been responsible for this (see Section 3.4). The expected circulation is observed in the non-magnetic run performed at the same numerical resolution as shown in the right-hand panel of Fig. 14.

3.4 Comparison with laminar viscous disc models

In addition to running the full MHD turbulent disc model, we have also run some two-dimensional (2D) laminar α disc models for

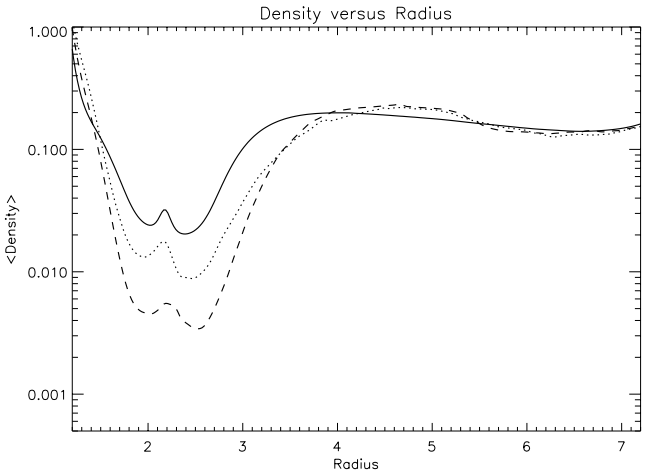

Figure 15. This plot shows the vertical midplane density distribution for the turbulent disc model (dotted line), a 2D laminar disc model with the Navier–Stokes $\alpha = 0$ (dashed line), and a 2D laminar disc model with $\alpha = 5 \times 10^{-3}$. It is clear that the gap for the 2D $\alpha = 0$ disc is the deepest, followed by the full turbulent disc model, with the 2D $\alpha = 5 \times 10^{-3}$ being the least deep and wide.

the purposes of comparison. A 2D model was run with $\alpha = 0$, along with an $\alpha = 5 \times 10^{-3}$ case. For initial conditions in these 2D models, we took the midplane density distribution of the 3D turbulent model just prior to the addition of the planet, switched off the magnetic field, and introduced the required value of α in the Navier–Stokes viscosity. The implementation of the Navier–Stokes viscosity is described in Nelson et al. (2000).

On a qualitative level, differences arise between the turbulent and laminar disc models. The most striking visual difference is that the spiral waves excited in the turbulent disc have a more 'blurred' appearance, whereas they appear to be more sharply defined in the laminar models; see Figs 8 and 16, and Nelson et al. (2000). Also, an inspection of the flow topology in the close vicinity of the planet shows some differences. In the turbulent disc case, there appears to be little sign of the usual circulating flow around the planet for material in the Hill sphere (see Fig. 14), whereas the laminar models do show the expected circulating flow pattern. This may indicate that magnetic linkage between the protostellar disc and the circumplanetary disc that forms when material flows into the protoplanets Hill sphere leads to magnetic braking. This effect may be highly significant for determining the accretion rate of gas on to the protoplanet through the circumplanetary disc, and indicates that accretion rates obtained from non-magnetic treatments of the problem may be quite different. We note, however, that higher-resolution simulations will be required to examine this effect in detail, and will be the subject of a future publication. In addition to these qualitative differences, there are also some important quantitative differences.

The azimuthally averaged surface density distributions for these models, plus the midplane density distribution for the turbulent model, are plotted in Fig. 15. Each of the models have been run for a total time of $\simeq$2050 time units, corresponding to $\sim$100 planetary orbits. It is clear that the $\alpha = 0.0$ 2D model (dashed line) has the deepest and widest gap, as expected. It is also apparent that the turbulent model (dotted line) has a deeper and wider gap than the 2D $\alpha = 5 \times 10^{-3}$ model, even though a volume averaged estimate for the underlying turbulent disc model yields an effective $\alpha \simeq 5 \times 10^{-3}$ (see figure 18 in Paper I). Thus, the turbulent model behaves as if it has a smaller α than reasonable estimates suggest it has. There are two probable reasons for this. First, a Navier–Stokes viscosity with anomalous viscosity coefficient provides a source of constantly acting friction in the disc, such that it can induce a steady mass flow into the gap region. The turbulence, however, does not operate as a constant source of friction that generates steady inflow velocities. Instead it generates large velocity fluctuations that may be much larger than the underlying inflow velocity arising from the associated angular momentum transport. Results presented in Paper I indicate that a process of time averaging the turbulent velocity field is required over long time periods before these fluctuations can be averaged out to reveal the underlying mass flow. The disc material in the vicinity of the planet experiences periodic high amplitude perturbations induced by the planet on a time-scale much shorter than the required averaging time-scale, so that the disc response is expected to differ from that in the case of a disc with Navier–Stokes viscosity. A second plausible reason for the apparently lower α is that the existence of the magnetic field in the turbulent disc allows for field lines to connect across the gap region, and to enable angular momentum transport across the gap. In this way, the magnetic field actually helps the planet to maintain the gap. Fig. 17 shows an example of how magnetic structures are able to extend across the gap and thus maintain communication across the gap region. The stresses associated with these structures lead to outwards angular momentum transport, and thus assist in maintaining the gap. However, it should be borne in mind that the above remarks apply to one particular simulation involving a thick disc with $H/r = 0.1$ and a protoplanet with 5 Jupiter masses. The ability of the ordered magnetic field to traverse the gap may be much less effective in a thinner disc in which the gap structure tends to be sharper and deeper. Also, the existence of significant disc material interior to the planet's orbit may assist this process, and in a model with an extensive inner cavity it may be less efficient. None the less, the differences in gap structure found here suggest that the accretion rate on to a protoplanet in an MHD turbulent disc is likely to be less than previous estimates based on laminar α disc models indicate (Bryden et al. 1999; Kley 1999; Lubow et al. 1999; Nelson et al. 2000; D'Angelo et al. 2002).

4 DISCUSSION AND CONCLUSIONS

We have presented a global MHD simulation of a turbulent disc interacting with a giant protoplanet in a fixed circular orbit. The disc model that we have considered (described in detail in Paper I) has $H/r = 0.1$, and in the absence of the protoplanet a volume and time averaged value of the stress parameter $\alpha = 5 \times 10^{-3}$. We have considered a protoplanet with 5 Jupiter masses which from previous work was expected to open and maintain a significant gap. Although the available computational resources have limited the parameters that could be adopted, we expect the essence of the disc–protoplanet interaction to be captured.

Using appropriate time averaged stress parameters and radial velocities, many of the phenomena seen in 2D laminar disc simulations could be demonstrated.

Spiral waves that produced an outward angular momentum flux through Reynolds stresses were launched by the protoplanet. As expected, the existence of the waves reduced the magnitude of the stresses provided by the MHD turbulence so reducing the associated outward angular momentum flow and thus maintaining the gap. A net outward angular momentum flow from the planet orbit to the disc was seen, which leads to inward migration of the protoplanet orbit on a time-scale expected from type II migration theory.

When compared with laminar disc models, with the same estimated α, the gap in the turbulent disc was found to be deeper

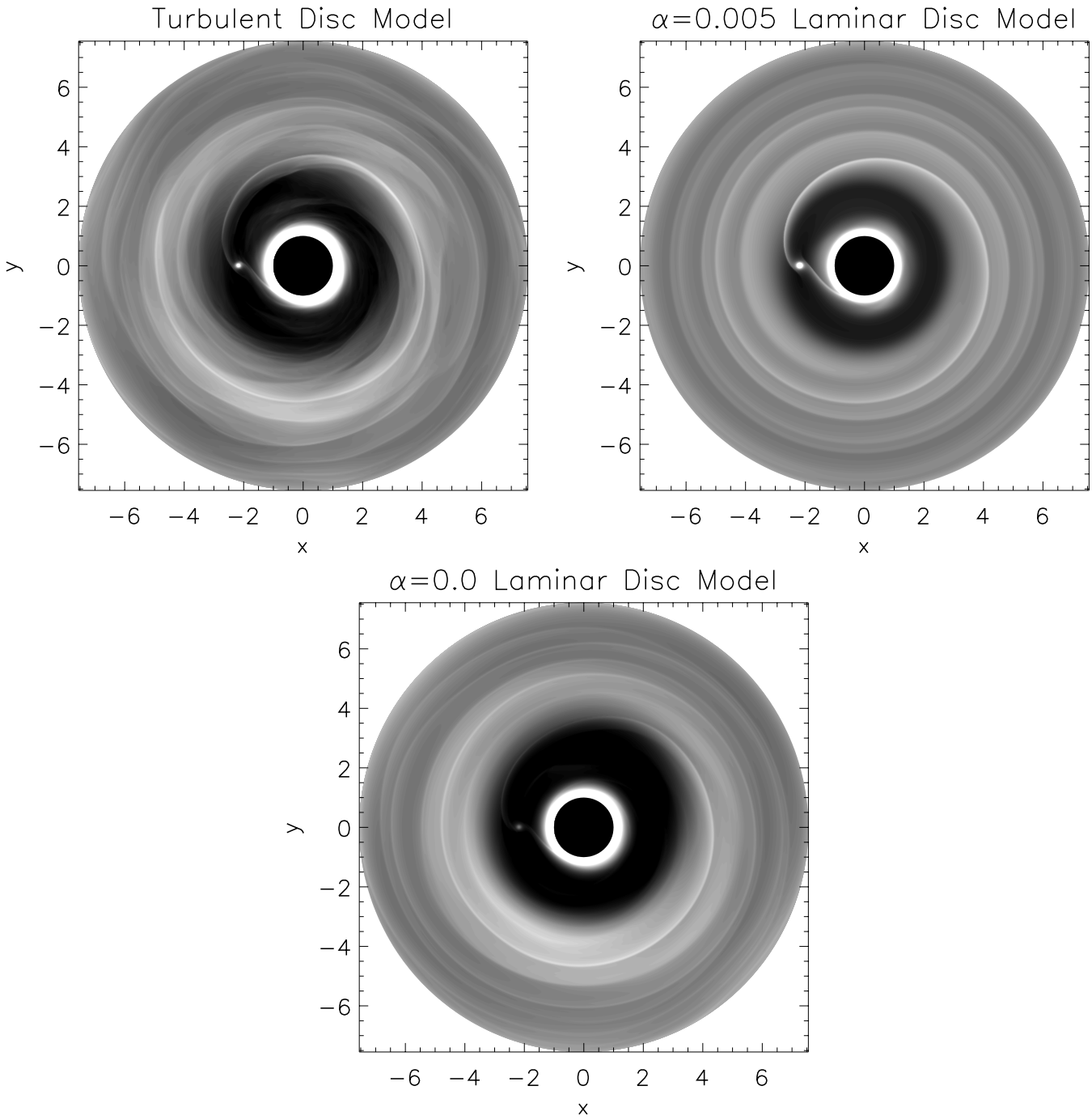

Figure 16. This plot shows the vertical midplane density distribution for the turbulent disc model (first panel), a 2D laminar disc model with the Navier–Stokes $\alpha = 5 \times 10^{-3}$ (second panel), and a 2D laminar disc model with $\alpha = 0$ (third panel). It is apparent that the spiral waves excited in the turbulent disc are 'blurred' by the effects of the turbulence, whereas those in the laminar disc model cases remain more sharply defined.

indicating that the turbulent disc behaved as if it possessed a smaller α. This was in spite of the fact that the turbulent disc appeared to be more effective at disrupting and dissipating the spiral waves. This behaviour may occur for two basic reasons. The first is that the turbulence does not provide a source of constantly acting friction in the disc, unlike a Navier–Stokes viscosity, and time averaging for significant periods is required before velocity fluctuations cancel out to reveal the underlying mass flow. The disc is periodically perturbed by the planet on time-scales shorter than those required for the time averaging, indicating that the disc response is likely to differ from a disc with Navier–Stokes viscosity operating. The second reason is that ordered magnetic structures were found to be able to cross the gap at azimuthal locations that were displaced from the planet by $\approx \pi$. Such a connection would enable an outward flux of angular momentum to flow across the gap and help to maintain it independently of the planetary torques, and so, as far as gap properties are concerned, making the disc appear to behave as if there was a smaller α. We also found no evidence for a persistent mass flow through the gap from the outer to inner disc but we emphasize that this may change if an extensive deep inner disc cavity can be produced or

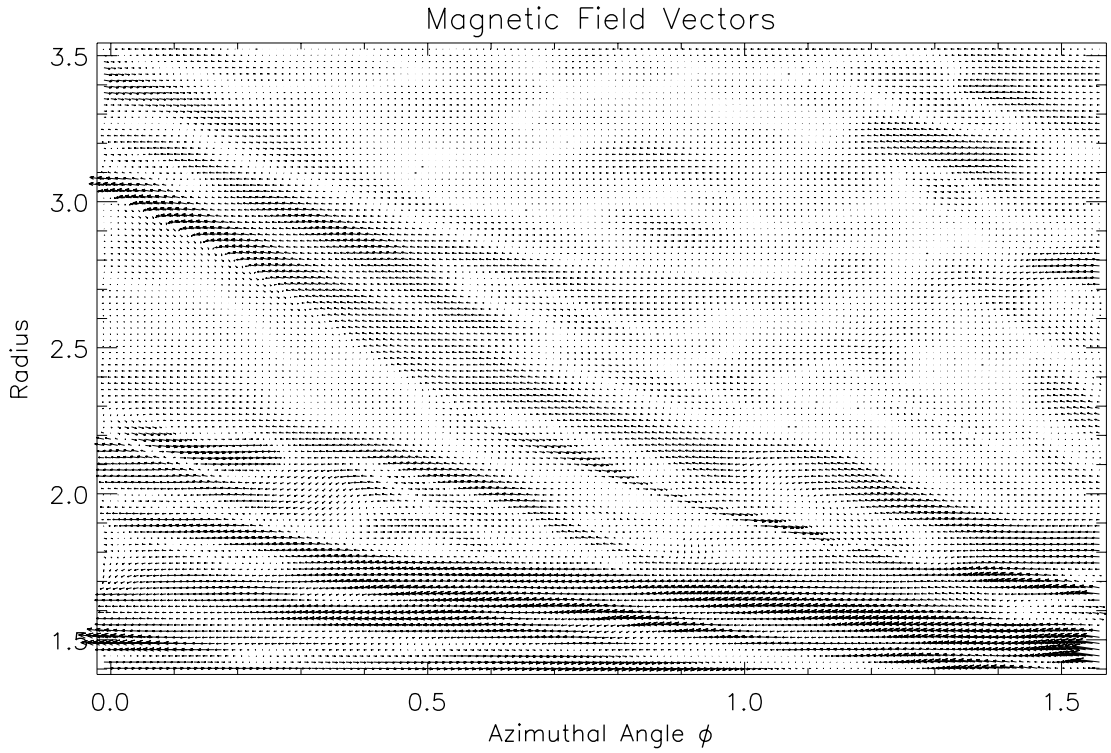

Figure 17. This plot shows magnetic field vectors (B_r and B_ϕ) plotted in the r–ϕ plane of the disc vertical midplane showing field structure in the gap region. It is evident that magnetic field lines are able to cross the gap (located between $r \simeq 1.8$ and $r \simeq 3.0$) and thus transmit torques between the two sides. This effect may be partially responsible for making the gap appear to resemble one formed in a laminar disc with smaller effective stress parameter α when a protoplanet is present in a turbulent disc. This is because these magnetic stresses are able to help maintain the gap. Note that features of this type tend to be less prevalent in the azimuthal domain near to the planet, but are more apparent in the regions that are close to π radians away from the planet.

if the disc is thinner. On the other hand, it may persist for smaller protoplanets which make weaker gaps and inner cavities.

The behaviour of the material bound to the planet was found to behave differently in the case of a magnetized disc, with the circulating material within the planetary Hill sphere apparently experiencing magnetic braking. This has implications for the structure and evolution of the circumplanetary disc that is expected to form during the latter stages of gas giant planet formation, and the mass accretion rate on to giant protoplanets. These issues require detailed investigation through additional simulations, and will be the subject of future publications.

ACKNOWLEDGMENTS

We acknowledge John Hawley, Steve Balbus, Adriane Steinacker and Caroline Terquem for useful discussions. The computations reported here were performed using the UK Astrophysical Fluids Facility (UKAFF).

REFERENCES

Armitage P. J., 1998, ApJ, 501, L189
Balbus S. A., Hawley J. F., 1991, ApJ, 376, 214
Balbus S. A., Papaloizou J. C. B., 1999, ApJ, 521, 650
Bodenheimer P., Pollack J. B., 1986, Icarus, 67, 391
Boss A. P., 2001, ApJ, 563, 367
Brandenburg A., Nordlund Å., Stein R. F., Torkelsson U., 1996, ApJ, 458, L45
Bryden G., Chen X., Lin D. N. C., Nelson R. P., Papaloizou J. C. B., 1999, ApJ, 514, 344
D'Angelo G., Henning T., Kley W., 2002, A&A, 385, 647
Gammie C. F., 1996, ApJ, 457, 355
Goldreich P., Tremaine S., 1979, ApJ, 233, 857
Hartmann L., Calvet N., Gullbring E., D'Alessio P., 1998, ApJ, 495, 385
Hawley J. F., 2000, ApJ, 528, 462
Hawley J. F., 2001, ApJ, 554, 534
Hawley J. F., Balbus S. A., 1991, ApJ, 376, 223
Hawley J. F., Stone J. M., 1995, Comput. Phys. Commun., 89, 127
Hawley J. F., Gammie C. F., Balbus S. A., 1996, ApJ, 464, 690
Kley W., 1999, MNRAS, 303, 696
Lin D. N. C., Papaloizou J. C. B., 1986, ApJ, 309, 846
Lin D. N. C., Papaloizou J. C. B., 1993, Protostars and Planets III. pp. 749–835
Lubow S. H., Seibert M., Artymowicz P., 1999, ApJ, 526, 1001
Marcy G. W., Cochran W. D., Mayor M., 2000, in Mannings V., Boss A. P., Russell S. S., eds, Protostars and Planets IV. University of Arizona Press, Tuscon, p. 1285
Mayor M., Queloz D., 1995, Nat, 378, 355
Nelson R. P., Papaloizou J. C. B., Masset F., Kley W., 2000, MNRAS, 318, 18
Papaloizou J. C. B, Lin D. N. C., 1984, ApJ, 285, 818
Papaloizou J. C. B., Nelson R. P., 2003, MNRAS, 339, 983 (Paper I, this issue)
Pollack J. B., Hubickyj O., Bodenheimer P., Lissauer J. J., Podolak M., Greenzweig Y., 1996, Icarus, 124, 62
Shakura N. I., Sunyaev R. A., 1973, A&A, 24, 337
Steinacker A., Papaloizou J. C. B., 2002, ApJ, 571, 413
Van Leer B., 1977, J. Comput. Phys., 23, 276
Vogt S. S., Butler R. P., Marcy G. W., Fischer D. A., Pourbaix D., Apps K., Laughlin G., 2002, ApJ, 568, 352
Ward W. R., 1997, Icarus, 126, 261
Ziegler U., Rüdiger G., 2000, A&A, 356, 1141

This paper has been typeset from a TEX/LATEX file prepared by the author.